JETP Letters, Vol. 81, No. 2, 2005, pp. 66–71. Translated from Pis'ma v Zhurnal Éksperimental'noĭ i Teoreticheskoĭ Fiziki, Vol. 81, No. 2, 2005, pp. 74–79.

Anomalies in Transport Properties in a Magnetically Ordered Region on a Kondo Lattice

S. S. Aplesnin

Kirenskiĭ Institute of Physics, Siberian Division, Russian Academy of Sciences, Akademgorodok, Krasnoyarsk, 660036 Russia

Siberian State Aerospace Academy, Krasnoyarsk, 660036 Russia

e-mail: apl@iph.krasn.ru

Received December 3, 2004; in final form, December 13, 2004

The temperature dependences of resistivity and thermal emf on a Kondo lattice are calculated using the spin-polaron approximation. The peaks and sign reversal points of thermal emf as a function of temperature and concentration below the temperature of the transition to the paramagnetic state are determined. The concentration region containing the metal–insulator transition below the Curie temperature and the shift of the upper spin-polaron band are calculated. © *2005 Pleiades Publishing, Inc.*

PACS numbers: 72.15.Qm; 72.20.–i

Intensive studies of manganites are stimulated by both the existence of the giant magnetoresistance effect and the possibility of application of these materials in spintronics. The magnetic ordering changes from the antiferromagnetic to ferromagnetic (FM) type, and the semiconductor–metal transition occurs at the critical concentration of the substitution of bivalent Ca^{2+} and Sr^{2+} ions for trivalent lanthanum ions [1–3]. Above the critical concentration ($x > x_c$), the resistivity in the FM region below the Curie temperature drops abruptly and is correctly described in the double exchange model [4]. In the vicinity of a concentration of $x \sim 0.5$, the metal–insulator transition is observed in $La_{0.5}Ca_{0.5-x}Ba_xMnO_3$ [5] below the Curie temperature T_{MI}/T_c = (x = 0) 0.87, (x = 0.1) 0.78, and (x = 0.2) 0.6. This transition can be interpreted using the phase-separation model. In other words, regions with the metal- and semiconductor-type conductivity exist due to small-radius polarons. However, the values of the activation energy calculated from the temperature dependences of the Seebeck coefficient $S(T)$ and resistivity differ from each other by an order of magnitude.

Available theories cannot explain an increase in the absolute value of thermal emf in double-layer manganites $RSr_2Mn_2O_7$ (R = La, Pr) in the helium temperature range [6]. The minimum observed in the $S(T)$ dependence for $La_{1.4}(Sr_{1-y}Ca_y)Mn_2O_7$ in the temperature interval 60 K < T < 150 K can be interpreted as a complex contribution from phonons and electrons to $S(T) = A/T + BT$. The sign reversal of the thermoelectric coefficient as a function of the temperature and concentration in manganites is explained by the presence of two types of carriers (electrons and holes) with different activation energies.

In this study, the above-mentioned effects are described in the Kondo-lattice model using spin polarons as charge carriers. The temperature and concentration ranges in which the Seebeck coefficient changes its sign and the metal–insulator transition occurs below the temperature of the transition to the magnetically ordered state are determined as functions of the spin-polaron band population and the Hund interaction parameter. The model proposed here differs from the double-exchange model, in which the hopping of Mn ions over e_g levels leads to the formation of ferromagnetic exchange, while hopping over t_{2g} states leads to the antiferromagnetic exchange between localized electrons. We assume that the motion of charged carriers takes place in the oxygen system and that the electron spin is polarized by the ordered arrangement of manganese spins due to the hybridization of oxygen and manganese ions. According to the x-ray diffraction data [7], the weights of the $3d^5L^1$ and $3d^6L^2$ states are approximately equal to 41 and 9%, which corresponds to one- and two-hole states. These states are located in the gap, and they can be treated as impurity bands near the chemical potential and described in the model of nearly free electrons. As applied to manganites, our model presumes that the substitution of the bivalent ion Sr^{2+} or Ca^{2+} for the trivalent La^{3+} ion leads to an increase in the concentration of holes on oxygen ions. Oxygen nonstoichiometry also forms the hole states on oxygen.

Spin-polaron excitations can be calculated in the framework of the Kondo-lattice model using the method proposed by Barabanov *et al.* [8]. The Hamiltonian has the form

$$H = H_0 + H_1 + H_2,$$

$$H_0 = \sum_{\mathbf{r},\mathbf{g}} t_{\mathbf{g}} a^+_{\mathbf{r}+\mathbf{g},\sigma} a_{\mathbf{r},\sigma} = \sum_{\mathbf{k}} \varepsilon_{\mathbf{k}} a^+_{\mathbf{k},\sigma} a_{\mathbf{k},\sigma},$$
$$H_1 = J \sum_{\mathbf{r},\sigma_1,\sigma_2} a^+_{\mathbf{r},\sigma_1} S^\alpha_{\mathbf{r}} \hat{\sigma}^\alpha_{\sigma_1,\sigma_2} a_{\mathbf{r},\sigma_2}, \quad (1)$$
$$H_2 = -\frac{1}{2}\sum_{\mathbf{r},\mathbf{g}} (I_1 S^\alpha_{\mathbf{r}+\mathbf{g}1} S^\alpha_{\mathbf{r}} + I_2 S^\alpha_{\mathbf{r}+\mathbf{g}2} S^\alpha_{\mathbf{r}}),$$

where summation is carried out over the cubic lattice sites, I_1 and I_2 are the exchange interactions between the nearest and next-to-nearest neighbors, $a^+_{\mathbf{k},\sigma}$ is the creation operator for an electron with the spin index $\sigma = \pm 1$, H_1 is the Hamiltonian of the *s–d* interaction, and $\hat{\sigma}^\alpha$ are the Pauli matrices with $\alpha = x, y, z$.

Let us write the equations of motion for the Green's functions describing the motion of the electron over oxygen ions. The electron spin interacts with the magnetically ordered spins of manganese ions. Using the random phase approximation, we close the system of equations for the Green's functions $\langle\langle a_{\mathbf{r},\sigma} | a^+_{\mathbf{r},\sigma}\rangle\rangle$ and $\langle\langle b_{\mathbf{r},\sigma} | a^+_{\mathbf{r},\sigma}\rangle\rangle$, where $b_{\mathbf{r}\sigma} = S^\alpha_{\mathbf{r}} \hat{\sigma}^\alpha_{\sigma,\sigma_1} a_{\mathbf{r},\sigma_1}$ and $\alpha = x, y$. These equations have the form

$$(\omega - \varepsilon_{\mathbf{k}}) G^1_{\mathbf{k}} = 1 + \frac{J}{2} G^2_{\mathbf{k}},$$
$$(\omega - e_{\mathbf{k}}) G^2_{\mathbf{k}} = J(1 + m - 2nm) G^1_{\mathbf{k}},$$
$$G^1_{\mathbf{k}} = \langle\langle a_{\mathbf{k},\sigma} | a^+_{\mathbf{k},\sigma}\rangle\rangle; \quad G^2_{\mathbf{k}} = \langle\langle b_{\mathbf{k},\sigma} | a^+_{\mathbf{k},\sigma}\rangle\rangle,$$
$$\varepsilon_{\mathbf{k}} = \varepsilon^0_{\mathbf{k}} + \frac{Jm}{4} - \mu, \quad (2)$$
$$\varepsilon^0_{\mathbf{k}} = -2(t_{xy}(\cos k_x + \cos k_y) + t_z \cos k_z),$$
$$e_{\mathbf{k}} = 2(z_1 c_1 + z_2 c_2)\varepsilon^0_{\mathbf{k}} + J\left(\frac{m}{2} + n\right)$$
$$+ m\left(\frac{z_1}{2} I_1 + \frac{z_2}{2} I_2\right) - \mu,$$
$$n = \langle a^+_\uparrow a_\uparrow + a^+_\downarrow a_\downarrow \rangle.$$

Here, $b_{\mathbf{k},\sigma}$, $a_{\mathbf{k},\sigma}$, and $G_{\mathbf{k}}$ are the Fourier transforms of the corresponding single-node operators and Green's functions, respectively, $c_{1,2} = \langle S^x_{\mathbf{r}} S^x_{\mathbf{r}+\mathbf{g}_{1,2}} + S^y_{\mathbf{r}} S^y_{\mathbf{r}+\mathbf{g}_{1,2}} \rangle$ is the spin–spin correlation function for transverse spin components, and z_1 and z_2 are the numbers of the nearest and next-to-nearest neighbors. All energies are measured from the chemical potential μ. The excitation spectrum has the form

$$\omega_{1,2}(\mathbf{k}) = \frac{1}{2}\left[\varepsilon_{\mathbf{k}} + e_{\mathbf{k}} \pm \sqrt{(\varepsilon_{\mathbf{k}} - e_{\mathbf{k}})^2 + J^2\left(\frac{1+m}{2} - nm\right)}\right]. \quad (3)$$

The chemical potential is calculated self-consistently for a given electron concentration n,

$$n = \frac{1}{N}\sum_{\mathbf{k}} \int d\omega f(\omega) \frac{1}{\pi} \mathrm{Im} G^1, \quad (4)$$

where $f(\omega) = (\exp(\omega/T) + 1)^{-1}$. Summation is carried out over 8×10^6 points in the first Brillouin zone. Here, we analyze the effect of magnetic ordering on the transport properties. For this reason, we consider the magnetic system in the adiabatic approximation to simplify the problem. The free energy expansion gives a power dependence for magnetization $m = m_0\sqrt{1 - T/T_c}$, where m_0 varies from $m_0 = 3.8\mu_B$ in $LaMnO_3$ [9] to $m_0 = 2.8\mu_B$ in $CaMnO_3$ [10]. The spin–spin correlation for the transverse spin components in the phase-transition region is about $c_{c1} \sim 0.1 m_0$ for $r = 1$ in accordance with Monte Carlo calculations in the classical Heisenberg model [11]. For $r = \sqrt{2}$, we have $c_{c2} \sim c_{c1}/\sqrt{2}$. The temperature dependence of c_1 and c_2 was described by the power function $c_{1,2} = c_{c1,2}(T/T_c)^2$ for $T < T_c$ and $c_{1,2} = c_{c1,2}(2 - T/T_c)^2$ for $T > T_c$. The typical values of exchange integrals, $I_1 \sim 1$ meV and $I_2 \sim 0.2$ meV [12], are three orders of magnitude smaller than the hopping integral and practically do not affect conductivity. The temperature of the transition from the magnetically ordered state to the paramagnetic phase in manganites varies in the interval 150 K $< T_c <$ 300 K, and we used the normalized quantity $T_c/t = 0.15$ in our calculations. The dynamic conductivity σ and the thermoelectric coefficient S were calculated using the Kubo–Greenwood formula [13]

$$\sigma = \frac{e^2}{T} L^{11},$$
$$S = \frac{1}{eT}\frac{L^{12}}{L^{11}},$$
$$L^{11} = T\sum_\sigma \sum_{\mathbf{k}} \int d\omega \left(-\frac{\partial f(\omega)}{\partial \omega}\right) A^2_\sigma(\mathbf{k}, \omega), \quad (5)$$
$$L^{12} = T\sum_\sigma \sum_{\mathbf{k}} \int d\omega \left(-\frac{\partial f(\omega)}{\partial \omega}\right) A^2_\sigma(\mathbf{k}, \omega)\omega,$$

where $A_\sigma(\mathbf{k}, \omega) = -(1/\pi)\mathrm{Im} G_\sigma(\mathbf{k}, \omega)$ is the spectral Green's function.

According to the calculations of the electron density functional *LDTA + U*, the gap width for the Mn–O

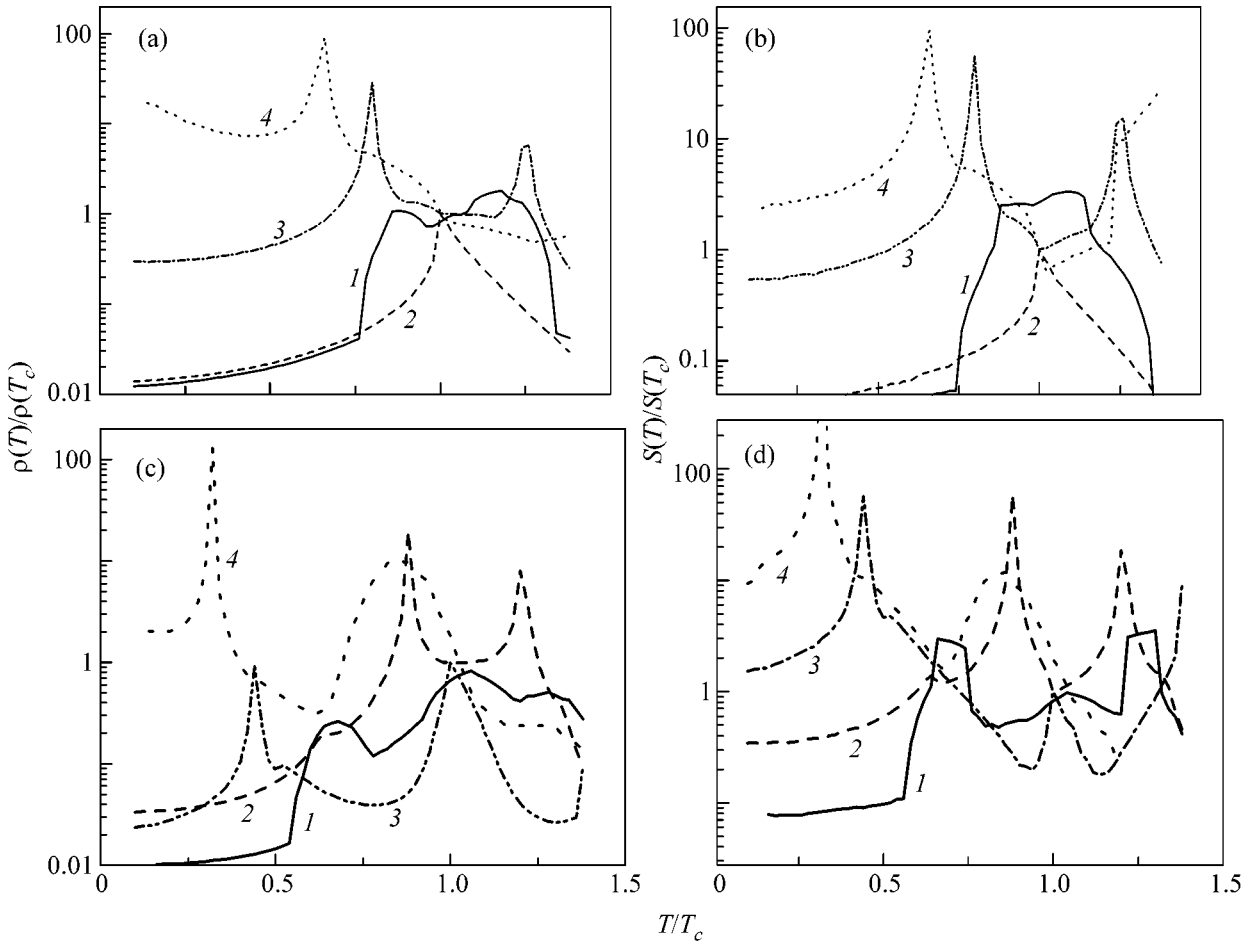

Fig. 1. (a, c) Resistivity $\rho(T)/\rho(T_c)$ and (b, d) thermal emf $S(T)/S(T_c)$ vs. the normalized temperature for J/t = (a, b) 8 and (c, d) 3 and x = (*1*) 0.1, (*2*) 0.3, (*3*) 0.5, and (*4*) 0.65.

charge transfer in $LaMnO_3$ is $(\varepsilon_p - \varepsilon_d) \sim 3.2$ eV [14] and the upper edge of the electron excitation band for oxygen lies below the chemical potential level by ~ 1 eV. The Mn–Mn electron orbitals do not overlap directly; the overlap integral of the wave functions between the Mn and O ions is $t(pd\sigma) = -1.99$ eV and $t(pd\pi) = 1.1$ eV, and $t(pp\sigma) = 0.7$ eV and $t(pp\pi) = -0.16$ eV for the O–O overlapping [15]. Electron excitations are localized on the manganese ions due to the large charge gap and Coulomb interaction, and nonstoichiometry facilitates the formation of holes with a higher mobility in the oxygen subsystem. The exchange interaction of hole spins on the oxygen ions with the spins on the manganese ions leads to the splitting of the hole band.

Numerical calculations of the transport coefficients by formulas (5) give two main temperature dependences of resistivity: a sharp decrease in the resistivity at a temperature of $T^* \le T_c$, $x < x_{c1}$ and at the metal–insulator transition at $T_{MI} < T_c$, $x > x_{c1}$. The corresponding $\rho(T)$ dependences are shown in Fig. 1. This behavior becomes clear from analysis of the spectrum of spin-polaron excitations and the density of states $g(\omega)$. In the vicinity of the Curie temperature, the two subbands overlap and form a peak of $g(\omega)$ in the overlap region. For low concentrations $x < x_{c1}$, the chemical potential lies at the bottom of the band. Upon cooling, the bands split and the chemical potential level gets into the van Hove region in the lower band. Since the conductivity is proportional to the density of states $N(0)$ at the chemical potential level, this behavior gives rise to a singularity in the $\rho(T)$ dependence. In the concentration range $x_{c1} < x$, the density $N(0)$ of spin-polaron excitations decreases sharply during the formation of long-range magnetic order, which corresponds to semiconductor-type conductivity. The transition temperature T_{MI} depends on the *s*–*d* interaction parameter and the band population and is determined by the shift of the chemical potential level from the upper subband to the lower one upon an increase in magnetization. The electron group velocity decreases sharply in this case, $v_k = \nabla\omega(k)$, and the conductivity is of the semiconductor type, because $\sigma \sim v_\mu^2 N(0)^2$, with a peak of $\rho_{max}(T_{MI})$ at the temperature at which the chemical potential level exactly coincides with the bottom of the upper subband.

Figure 2a shows the dispersion curves in the [111] direction for two temperatures: $T < T_{MI}$ and $T > T_{MI}$. The density of states remains virtually unchanged at these temperatures (Fig. 2b). Band splitting increases with the *s–d* interaction parameter, and higher electron concentrations are required for the chemical potential to lie in the upper band. This leads to an increase in the metal–insulator transition temperature T_{MI}, which is observed in Fig. 1.

The calculated temperature dependences of thermal emf are in qualitative agreement with the conductivity type. Namely, the Seebeck coefficient for $\rho(T)$ of the metal and semiconductor types increases and decreases, respectively, with increasing temperature (see Fig. 1). In the quasi-two-dimensional case, this correlation is violated. Figure 3 shows the $\rho(T)$ and $S(T)$ curves for the anisotropic hopping parameters t_z/t_{xy} = 0.1, which are typical of double manganites $LaSr_2Mn_2O_7$ [16]. The thermal emf attains its minimum in the region of the transition to the paramagnetic state and changes its sign from positive to negative both in temperature and in concentration for $x_c < x$. The sign reversal of $S(T)$ is due to the specific behavior of the density of states in the vicinity of the chemical potential, which is shown in Fig. 2. For example, the densities of states for $\omega > 0$ and $\omega < 0$ in the energy range close to the Curie temperature differ from each other by several times, while the density of states $g(\omega)$ in the low-temperature range for constant parameters x and J is practically symmetric with respect to the chemical potential in the interval $\Delta\omega \simeq 2T_c$. Doped manganites are semimetals in accordance with the spin-resolution photoemission data [17]. The calculated $\rho(T)$ and $S(T)$ dependences qualitatively explain two peaks in the temperature dependence of the thermal emf with a minimum in the vicinity of the Curie temperature in $La_{1.2}Sr_{1.8}Mn_2O_7$ [18] and the sign reversal of the thermal emf as a function of the temperature in $La_{1-x}Ca_xMnO_3$ for $x = 0.32$ [19]. The region in which the thermal emf changes its sign in the magnetically ordered state at $T < T_c$ strongly depends on the dimensionality of the space and is shown on the *x–J* phase diagram in Fig. 4a.

The conductivity calculated using the dynamical mean field method disregarding the dependence of the electron self-energy on the quasimomentum [4] decreases rapidly with increasing magnetization $\rho(m)/\rho(m = 0) = 1 - Cm^2$. In this approximation, it is impossible to obtain a metal–insulator transition in temperature for $T_{MI} < T_c$.

In our model, we assume that conduction is realized over oxygen ions and that the upper edge of the band shifts towards high frequencies at $T < T_c$, where $t_z = t_{xy}$, and the shift increases with concentration (see Fig. 4). The intrinsic absorption edge corresponding to a gap of approximately 1 eV is determined from the diffuse reflection spectra for $La_{0.9}Sr_{0.1}MnO_3$ [20]. In the temperature range from T_c = 155 K to 140 K, the intrinsic absorption edge shifts by a giant value of about 0.4 eV [20]. Figure 4 shows the theoretical and experimental results, which are in satisfactory agreement. According

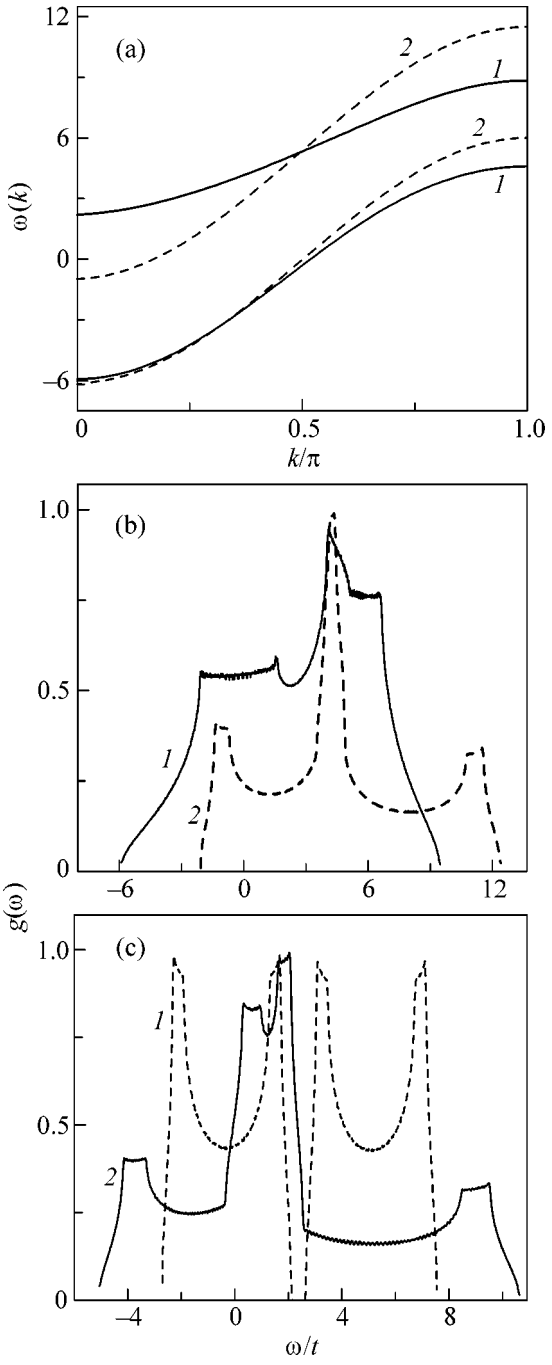

Fig. 2. (a) Spectrum of spin-polaron excitations $w_{[111]}(k)$ at temperatures T/T_c = (solid curves) 1/3 and (dashed curves) 0.47 for $J/t = 3$ and $x = 0.5$. (b, c) Density of states of spin-polaron excitations for $J/t = 3$ and (b) x = (*1*) 0.5 and (*2*) 0.25, T/T_c = (*1*) 0.4 and (*2*) 0.8, and t_z/t_{xy} = (*1*) 1 and (*2*) 0.1; and (c) $x = 0.5$, $t_z/t_{xy} = 0.1$, and T/T_c = (*1*) 0.55 and (*2*) 0.88.

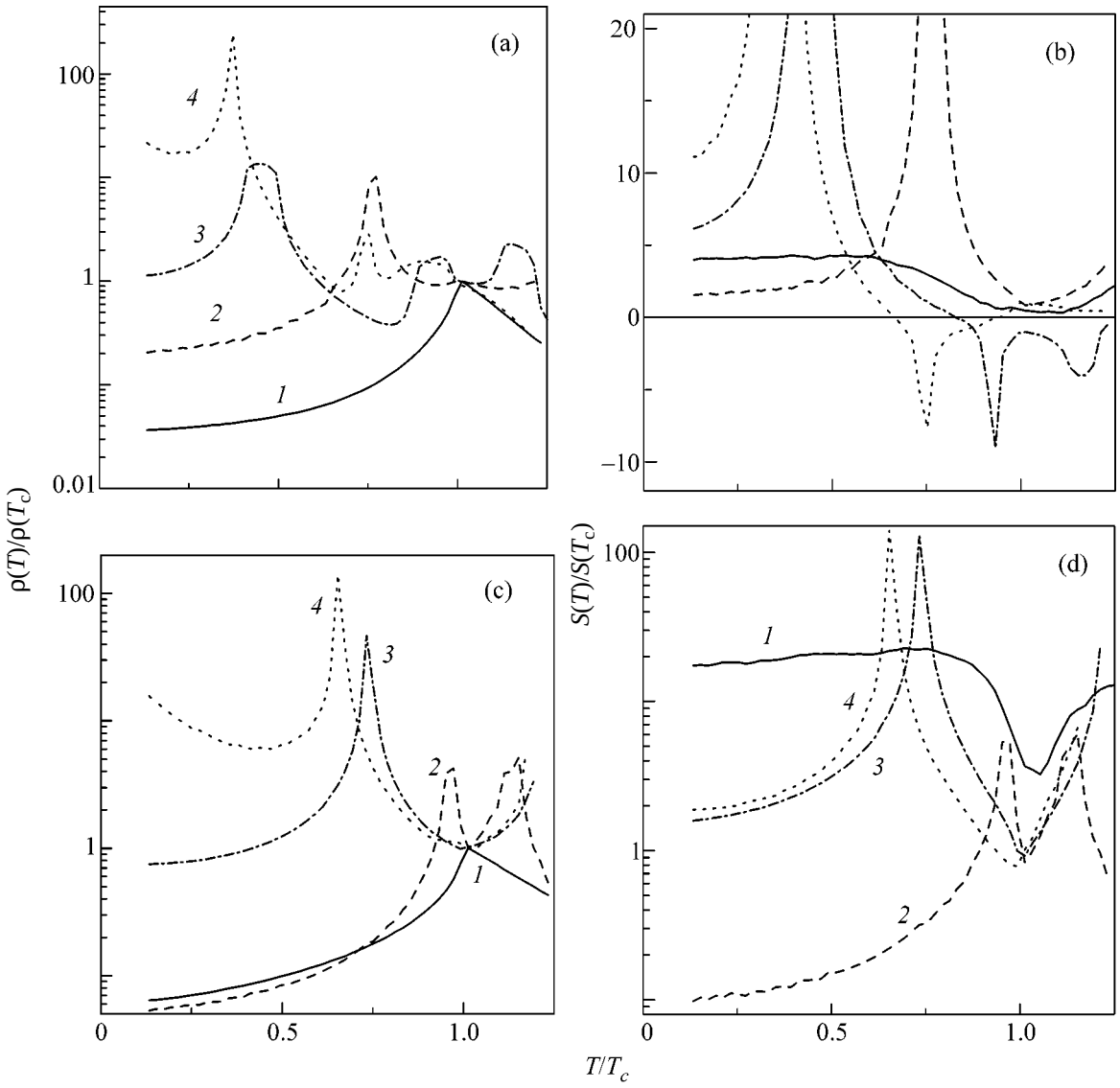

Fig. 3. (a, c) Resistivity and (b, d) thermal emf in a quasi-two-dimensional system vs. the normalized temperature for $t_z/t_{xy} = 0.1$, J/t = (a, b) 3 and (c, d) 6, and x = (*1*) 0.1, (*2*) 0.3, (*3*) 0.5, and (*4*) 0.65.

to Demin *et al.* [20], the red shift of the gap is associated with the shift of the top of the valence band and rules out the electron-phonon interaction mechanism in view of its smallness, because the isotopic effect is small in this band [21].

The application of our spin-polaron model for describing the transport properties of manganites is restricted to metallic compounds with a long-range or short-range ferromagnetic order in the vicinity of the Curie temperature. In the framework of this model, it is impossible to obtain the temperature dependence of resistivity for nonferromagnetic doped manganites. The temperature and magnetic-field dependences of resistivity in these compounds are described in the inhomogeneous-state model [22], in which a ferromagnetic polaron is pinned at an impurity center or moves very slowly in the insulator matrix. The main contribution to transport in this case comes from electron hopping from one stationary ferron to a neighboring one. The resistivity in the phase-separated region is governed by the Mott law $\rho(T) \sim T\exp(A/2k_BT)$, where the energy barrier height $A \sim e^2/\varepsilon_0 R_f$ depends on the ferron radius R_f. Our model can be used in the concentration range $0.18 < x < 0.5$ for $La_{1-x}A_xMnO_3$, A = Ca, Sr [23] and in the range $0.2 < x < 1$ for $La_{2-2x}Sr_{1+2x}Mn_2O_7$ [16] and other ferromagnetic compounds exhibiting the metal–insulator transition in temperature.

Thus, the interaction of free charge carriers with localized spins in the range of high concentrations leads to a resistivity peak below the Curie temperature. The peak observed in the $\rho(T)$ dependence for manganites with the FM ordering is also successfully explained in

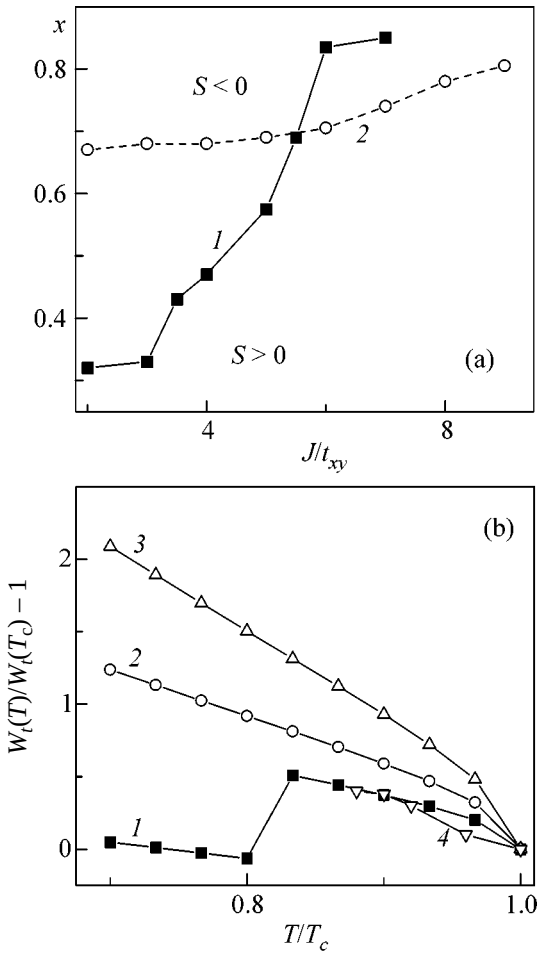

Fig. 4. (a) Lines on the x–J phase diagram separate the upper region with the sign reversal of thermal emf at $T < T_c$ from the lower region with $S(T) > 0$ for t_z/t_{xy} = (*1*) 0.1 and (*2*) 1. (b) Normalized shift of the upper edge of the spin-polaron excitation band $W_t(T)/W_t(T_c) - 1$ as a function of the normalized temperature T/T_c for $J/t = 8$, x = (*1*) 0.15, (*2*) 0.25, (*3*) 0.35, and (*4*) $La_{0.9}Sr_{0.1}MnO_3$ [20].

the spin polaron model as in the case of lower concentrations. The sign reversal in the temperature dependence of the Seebeck coefficient, as well as in its concentration dependence, also fits the spin-polaron excitation model without including the phonon mechanism or phase separation. The splitting and shift of the spin-polaron band satisfactorily correlate with the shift of the top of the valence band determined from the diffuse scattering data for manganites.

REFERENCES

1. É. L. Nagaev, Usp. Fiz. Nauk **166**, 833 (1996) [Phys. Usp. **39**, 781 (1996)].
2. L. P. Gor'kov, Usp. Fiz. Nauk **168**, 666 (1998) [Phys. Usp. **41**, 589 (1998)]; M. Yu. Kagan and K. I. Kugel', Usp. Fiz. Nauk **171**, 577 (2001) [Phys. Usp. **44**, 553 (2001)].
3. Yu. A. Izyumov and Yu. N. Skryabin, Usp. Fiz. Nauk **171**, 121 (2001) [Phys. Usp. **44**, 109 (2001)].
4. N. Furukawa and K. Hirota, Physica B (Amsterdam) **241–243**, 780 (1997).
5. H. Wakai, J. Phys.: Condens. Matter **13**, 1627 (2001).
6. S. Chatterjee, P. H. Chou, C. F. Chang, *et al.*, Phys. Rev. B **61**, 6106 (2000).
7. D. D. Sarma, O. Rader, T. Kachel, *et al.*, Phys. Rev. B **49**, 14238 (1994).
8. A. F. Barabanov, L. A. Maksimov, and A. V. Mikheenkov, Pis'ma Zh. Éksp. Teor. Fiz. **74**, 362 (2001) [JETP Lett. **74**, 328 (2001)].
9. M. B. Salamon and M. Jaime, Rev. Mod. Phys. **73**, 583 (2001).
10. W. E. Pickett and D. J. Singh, Phys. Rev. B **53**, 1146 (1996).
11. S. S. Aplesnin, Fiz. Met. Metalloved. **63**, 190 (1987).
12. D. Feinberg, P. Germain, M. Grilli, and G. Seibold, Phys. Rev. B **57**, R5583 (1998).
13. K. Nagai, T. Momoi, and K. Kubo, J. Phys. Soc. Jpn. **69**, 1837 (2000).
14. A. Chainani, M. Mathew, and D. D. Sarma, Phys. Rev. B **47**, 15397 (1993).
15. P. Mahadevan, N. Shanthi, and D. D. Sarma, Phys. Rev. B **54**, 11199 (1996).
16. Y. Liu, L. Sheng, D. Y. Xing, and J. Dong, J. Phys.: Condens. Matter **10**, 9747 (1998).
17. V. Yu. Irkhin and M. I. Katsnel'son, Usp. Fiz. Nauk **164**, 705 (1994) [Phys. Usp. **37**, 659 (1994)].
18. J. S. Zhou, J. B. Goodenough, and J. F. Mitchell, Phys. Rev. B **58**, R579 (1998).
19. A. Asamitsu, Y. Moritomo, and Y. Tokura, Phys. Rev. B **53**, R2952 (1996); K. M. Kojima, Y. Fudamoto, M. Larkin, *et al.*, Phys. Rev. Lett. **78**, 1787 (1997).
20. R. V. Demin, L. I. Koroleva, and A. M. Balbashov, Pis'ma Zh. Éksp. Teor. Fiz. **70**, 303 (1999) [JETP Lett. **70**, 314 (1999)].
21. G. M. Zhao, K. Conder, H. Keller, and K. A. Müller, Nature **381**, 676 (1996).
22. A. L. Rakhmanov, K. I. Kugel, Ya. M. Blanter, and M. Yu. Kagan, Phys. Rev. B **63**, 174424 (2001); K. I. Kugel', A. L. Rakhmanov, A. O. Sboĭchakov, *et al.*, Zh. Éksp. Teor. Fiz. **125**, 648 (2004) [JETP **98**, 572 (2004)].
23. J. Hemberger, A. Krimmel, T. Kurz, *et al.*, Phys. Rev. B **66**, 094 410 (2002).

Translated by N. Wadhwa